DOI: 10.2507/36th.daaam.proceedings.xxx

DESIGN OF A HANGING PARALLEL ROBOT FOR PLASTERING BRICK WALLS IN CONSTRUCTION

Jorge Francisco Aznar-Ortega, Adrián Peidró, Luis Payá & Óscar Reinoso





This Publication has to be referred as: Katalinic, B[ranko]; Park, H[ong] S[eok] & Smith, M[ark] (2025). Title of Paper, Proceedings of the 36th DAAAM International Symposium, pp.xxxx-xxxx, B. Katalinic (Ed.), Published by DAAAM International, ISBN 978-3-902734-xx-x, ISSN 1726-9679, Vienna, Austria DOI: 10.2507/36th.daaam.proceedings.xxx

Abstract

In the construction industry, plastering brick walls is necessary for structural and aesthetic reasons, as it provides smooth and even surfaces for decoration, protects against moisture and weather damage, and enhances the durability of the walls. Traditionally, plastering has been executed by human workers. When the wall is so tall that it spans several stories, it is necessary to use scaffolds, gondolas or ropes from which humans hang while they manually perform the plastering, which endangers their lives due to the risk of falling. To avoid this and automate the process, some plastering robots and machines have been proposed in the last years, but they have limitations such as limited vertical reach or the necessity of resting on horizontal surfaces at the bottom of the wall. To overcome these limitations, we propose a new robot consisting of a planar parallel mechanism that hangs from cables, increasing vertical reach and avoiding the need of resting horizontally. In this paper, we demonstrate the kinematic design, and the workspace and force analysis to guarantee that sufficient pressure is applied stably to the wall during plastering while cables remain taut.

Keywords: Wall plastering; parallel robot; cable robot; workspace; force analysis.

1. Introduction

Construction is still a sector with low levels of automation and is not free of hazards for operators [1], [2]. Many of the tasks in this area are labour-intensive, require precision and skill and consist of repetitive movements. In addition, the demanding conditions and unclean working environment have led to a decreasing number of skilled workers willing to engage in this field. Therefore, robots need to be developed to alleviate the human workload and compensate for the shortage of personnel in construction [3], [4], [5], [6].

One of the tasks commonly performed in construction is the plastering of vertical walls. This type of work is still mostly done manually. For small buildings, plastering can be done from the ground or small heights and does not pose a significant hazard for the labourers. However, for larger buildings with high walls, it is necessary for workers to hang from the facade or work from cranes or scaffolding, which entails a risk of falling.

There are currently robots for plastering, both for research and commercial use. Some of them make use of technologies such as convolutional neural networks (CNN) to detect defects in plasterwork and correct them [7], [8]. However, most existing robots consist of a trolley with a retractable mast that extends vertically up the wall to perform

the plastering [9], [10], [11]. This type of robot model has limitations that make it unsuitable for some cases, such as when the height of the surface to be plastered is greater than the range achievable by the robot's mast. Likewise, these robots need horizontal support to hold up the trolley, which is a problem when the lower part of the wall is not horizontal, but another adjacent roof or other sloping surface.

In summary, despite the existence of some robots that can perform the plastering task, their use is limited to certain workplace conditions. For this reason, the design and creation of a new robot that can be used in a wider range of situations is beneficial to help alleviate the lack of workers and to avoid dangerous situations for operators and occupational accidents in the construction sector. The solution proposed in this article, which will be described in more detail in Section 2, consists of a hanging robot with a parallel robot on its gondola and an adhesion arm. This configuration overcomes the limitations of previous robots, such as limited vertical reach and the need to rest on a horizontal surface, among others.

The remainder of this paper is organized as follows: Section 2 describes in detail the configuration of the robot, Section 3 presents its kinematic and workspace analysis. Next, Section 4 focuses on force analysis. Later, Section 5 explains the singularity analysis. Following, Section 6 analyses the results of these analyses and, finally, Section 7 draws conclusions and suggests future lines of work.

2. Description of the proposed robot for plastering

The wall plastering robot presented in this paper is shown in Figure 1. It consists of a gondola suspended by cables $(C_1 \text{ and } C_2)$ that moves vertically along the walls of buildings. The cable-driven system allows flexible positioning at different heights. Mounted on the gondola there is a parallel robotic mechanism (Figure 2) with three degrees of freedom $(P_1, P_2 \text{ and } P_3)$, responsible for adjusting both the location and orientation of the scraper (triangle formed by points A_1 , A_2 and A_3). The use of a parallel structure offers high rigidity, which is important for achieving uniform plastering across the entire surface of the wall.

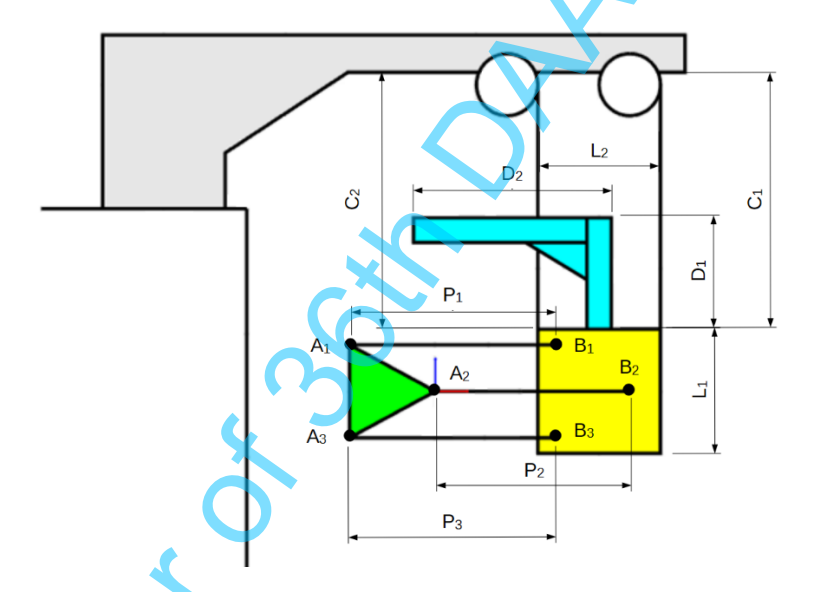


Fig. 1. Representation of the plastering robot

Since the support cables only control vertical movement and do not exert any force towards the wall, the reaction force generated during the application of the mortar could push the robot away from the surface. To solve this, the robot incorporates a wall adhesion mechanism, preferably by suction, which ensures that the robot remains in contact with the wall while operating (bars of length D_1 and D_2 , where D_2 is extensive/retractile). This mechanism will maintain constant pressure during application, preventing the robot from malfunctioning.

The robot's operating sequence begins with its placement at the desired height. Once there, the adhesion system is activated to secure the robot to the wall. When stable contact is established, the mortar applicator adjusts to the required position and orientation to begin the plastering process. The robot then covers the entire accessible surface from that height. Once the plastering in that area is complete, the adhesion mechanism disengages from the wall, and the robot repositions itself via the cables to a new area to continue the task. This sequence is repeated until the entire target surface is plastered.

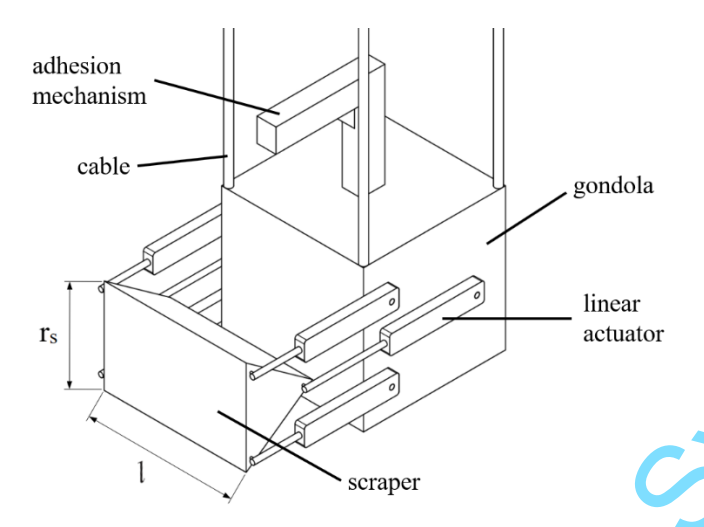


Fig. 2. Location of the robot's parallel mechanism

3. Kinematics and workspace

When defining the location of the robot's elements, three different reference systems have been used, as shown in Figure 3. The first of these is the fixed inertial system, which is defined by the X and Y axes. The origin of the second system is located on the gondola, with its axes being X' and Y'. Finally, the third reference system is fixed on the scraper, with axes X'' and Y'' and its orientation φ .

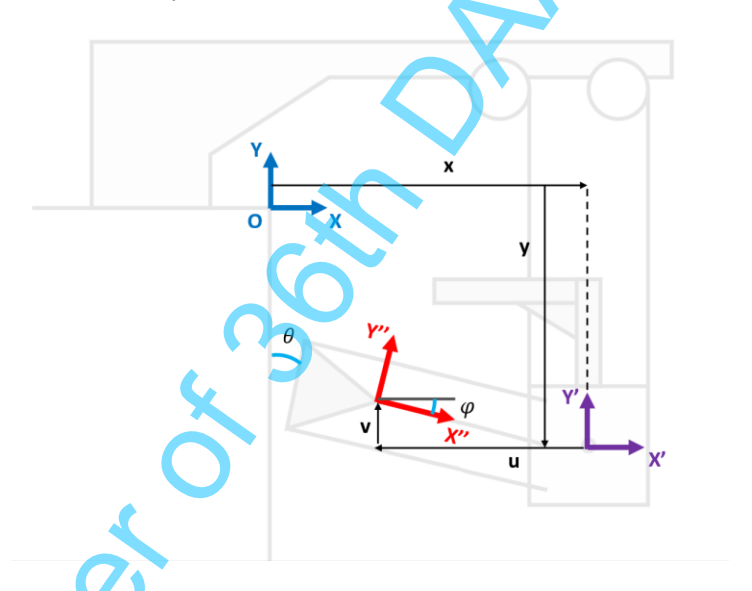


Fig. 3. Location of reference systems

For the robot presented in this paper, the kinematic input variables are the lengths of the prismatic actuators: P_1 , P_2 and P_3 . Likewise, the output variables (or platform pose) are the coordinates of the platform reference point (u, v) and its orientation relative to the carriage (φ) .

There are two types of kinematic calculations. First, the direct kinematics of the robot is based on determining the position and orientation of the end effector (scraper) from the known values of the actuator lengths. The solution is obtained by solving a sixth-degree polynomial, as explained in [12]. However, the calculation of direct kinematics will not be necessary for this work, so it will not be developed here.

Secondly, inverse kinematics consists of calculating the prismatic lengths of the actuators based on a desired pose (position and orientation) of the end effector. This calculation is quite simple and is more relevant because it is the most useful in practice. To calculate inverse kinematics, the following data is used as a starting point:

• Fixed points on the gondola:

$$B_i = \begin{bmatrix} B_{i_x} \\ B_{i_y} \end{bmatrix} \quad i = 1, 2, 3$$

• Points of the end effector, expressed in its local system:

$$A_{i_local} = \begin{bmatrix} A_{i_{x_local}} \\ A_{i_{y_local}} \end{bmatrix} \quad i = 1, 2, 3$$

• Platform pose:

$$p = \begin{bmatrix} u \\ v \end{bmatrix}$$
, angle: φ

• Rotation matrix:

$$R(\theta) = \begin{bmatrix} \cos(\varphi) & -\sin(\varphi) \\ \sin(\varphi) & \cos(\varphi) \end{bmatrix}$$

Thus, the end effector points represented in the reference system of the gondola (X' Y') are obtained using the following expression:

$$A_{i_global} = \begin{bmatrix} \cos(\varphi) & -\sin(\varphi) & u \\ \sin(\varphi) & \cos(\varphi) & v \\ 0 & 0 & 1 \end{bmatrix} \begin{bmatrix} A_{i_{x_local}} \\ A_{i_{y_local}} \\ 1 \end{bmatrix} \quad i = 1, 2, 3$$

$$(1)$$

Given the start and end points of the prismatic actuators in gondola coordinates, the inverse kinematics is solved using this formula:

$$P_i = \|A_i - B_i\| \quad i = 1, 2, 3 \tag{2}$$

Finally, the calculation of the robot's range of motion is discussed. To do this, the constant orientation workspace is defined, which consists of the positions (x, y) that the scraper can reach for a fixed orientation and given minimum (P_{min}) and maximum (P_{max}) piston lengths $(P_{min} \le P_i \le P_{max})$. To perform this analysis, it is necessary to determine the range of orientations compatible with the plastering task, which requires incorporating the force analysis presented in the following section.

4. Static force analysis

To begin solving the static force analysis, the formulation described in [13] is adopted. Figure 4 illustrates the variables that will be used in (3), (4) and (5). First, the angle formed by the scraper and the wall is called θ . Likewise, the support force of the scraper on the mortar is represented by F. On the other hand, the compaction force of the mortar is indicated as N. Finally, the variables f_l and f_w are the friction force of the scraper on the mortar and of the wall on the mortar, respectively.

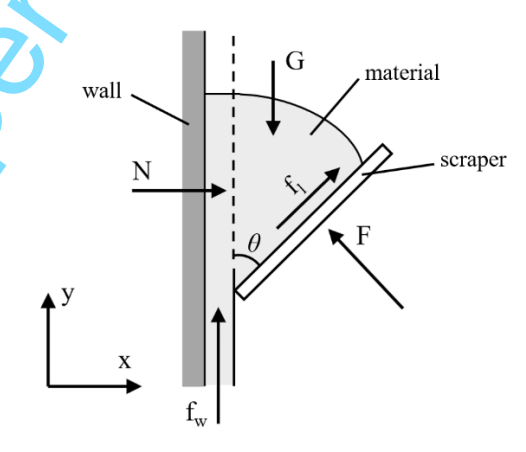


Fig. 4. Physical model for scraper plastering. Adapted from [13]

Therefore, the equations used to obtain the valid range of orientations for the plastering task are as follows:

$$G = \frac{1}{4} \cdot r_s^2 \cdot l \cdot \rho \cdot g \cdot \sin(2\theta)$$
 (3)

$$F \cdot \cos(\theta) = N + f_l \cdot \sin(\theta)$$

$$F \cdot \sin(\theta) + f_w + f_l \cdot \cos(\theta) = G$$
(4)

Since $f_w = \mu_w \cdot N$, $f_l = \mu_l \cdot F$, it can be derived:

$$N = \frac{G}{(1 - \mu_l \cdot \mu_w) \cdot \sin(\theta) + (\mu_l + \mu_w) \cdot \cos(\theta)} \cdot (\cos(\theta) - \mu_l \cdot \sin(\theta))$$
 (5)

The constants are the density of the mortar (ρ) , the force of gravity (g), the coefficient of friction between the wall and the mortar (μ_w) and the coefficient of friction between the scraper and the mortar (μ_l) . Also, the width (r_s) and length (l) of the scraper (Figure 2).

If it is considered that the compaction force, N, must be greater than 100 N, an inequality that depends on the angle θ is obtained. By solving this inequality, the valid angles (θ) for the plastering task (Figure 5), the values of the forces N and F, as well as the friction forces f_1 and f_w are obtained.

It should be noted that the range of valid angles obtained is small (from 16° to 37°), but comparable in amplitude to that of [13], which was from 12° to 37°. This range is reasonable because it must be considered that the inclination of the scraper is limited by the conditions of the task, since it cannot be too horizontal or too vertical to perform the plastering.

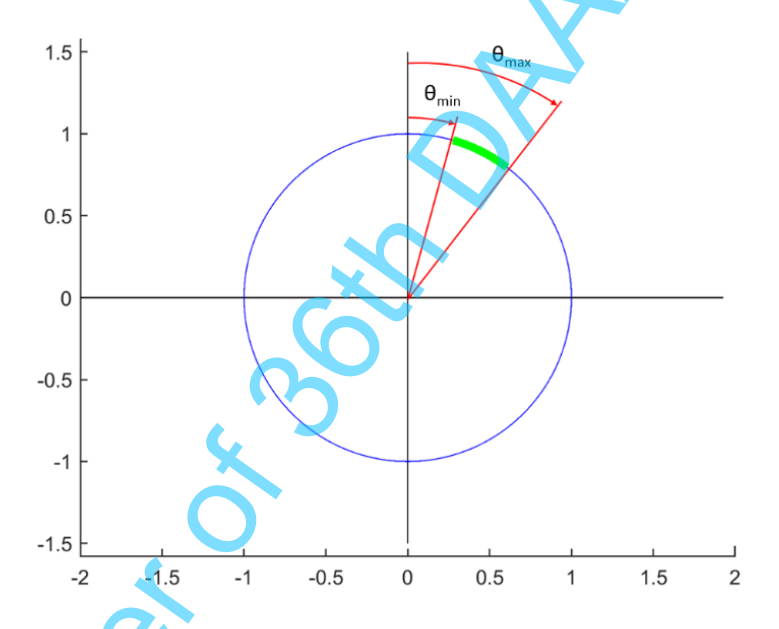


Fig. 5. Range of valid values for theta angle (θ)

Next, based on the data represented in Figure 6, the equations for the static equilibrium of the robot (6), (7) and (8) are established, considering all forces and moments. For the calculation of the moments, the reference point is indicated by the letter A. Known values include the adhesion force ($F_{adhesion}$), some distances and the weight of the gondola, which have been reasonably estimated. The rest of the variables involved (F_x , F_y , F_y , F_y , F_y , F_y , depend on the position and orientation of the scraper, so their values will change according to these variables. Finally, the unknown variables are the reaction force ($F_{reaction}$) and the cable tensions (F_y) and F_y).

$$F_{reaction} = F_{adhesion} - F_x \tag{6}$$

$$P = T_1 + T_2 + F_y (7)$$

$$M_1 + F_x \cdot d_{Fx} + T_2 \cdot d_{T2} = F_y \cdot d_{Fy} + T_1 \cdot d_{T1}$$
(8)

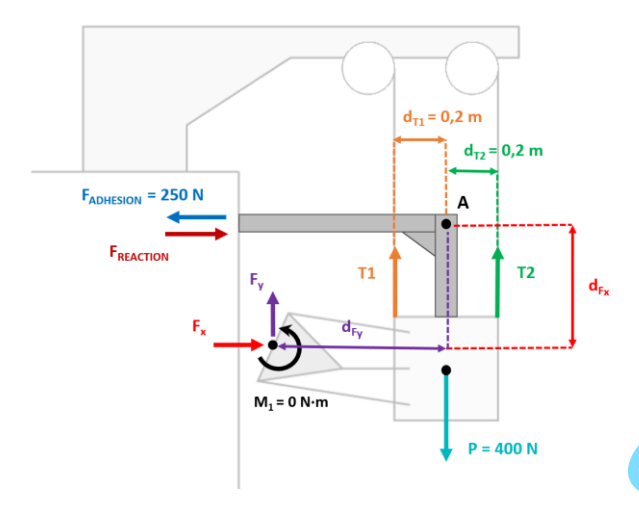


Fig. 6. Diagram of forces and moments on the robot

Solving the unknown variables in the above system of equations yields a table of results (one result for each angle θ) that meets the constraints. The values obtained must then be checked, as only those greater than zero are valid. This is because the cables can only withstand tensile forces and the reaction force can never be negative, as this would mean that it is exerting a force against the wall.

5. Singularity analysis

A singularity is a geometric configuration of a robot in which control over its movements or the forces it can transmit is lost. In parallel robots, these singularities occur when the geometry of the mechanism causes the end effector to move in a direction not controlled by the actuators, or when the actuators are unable to generate certain movements required of the end effector.

Mathematically, singularities are detected when the Jacobian matrices that relate velocities/displacements between actuators and end effectors lose rank or, in other words, their determinant is zero or almost zero.

To analyse the singularities of this robot, we will first determine the expression of its Jacobian matrix and then calculate the determinant for each of the valid points in the workspace. The Jacobian matrix that will be considered is formed by the derivatives of the right-hand side of (2) with respect to (u, v, φ) . If there were sign changes between the points in the workspace, this would mean that those points would be singular. Otherwise, the robot would have no singularities and could be controlled at all points in the workspace.

6. Results

Based on the values of angle θ obtained in the previous section, an algorithm has been programmed in MATLAB that performs a sweep of the positions (x, y) of the end effector with a step of 0.01 between u = [-2, -0.5] and v = [-1.6, 1.6]. This range of values has been chosen because it covers the space between the wall and the robot, ensuring that the scraper does not come into contact with other objects. The representation of the point mesh that will be traversed by point A_2 of the scraper is shown in Figure 7.

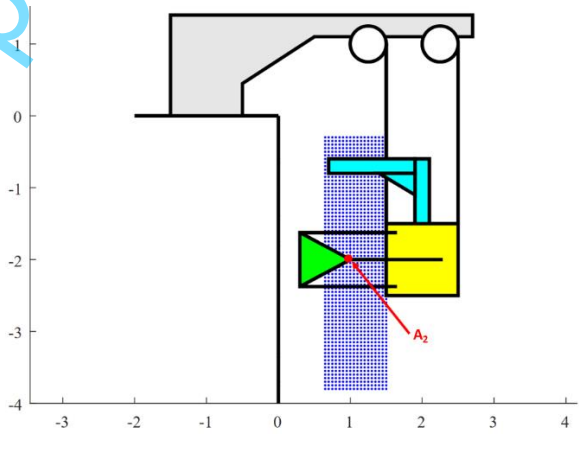


Fig. 7. Grid of points

For each point (x, y), the inverse kinematics is solved, as explained in Section 3, obtaining the lengths that the pistons should have in each case. For the initial design of the robot, commercial pistons with the following characteristics will be chosen: stroke of 20 cm, minimum length of 40 cm and maximum of 60 cm. Therefore, it must be verified that the lengths obtained through inverse kinematics are within these values. If the lengths of the three pistons are in the specified range, before qualifying the point as valid, a static check must be performed to determine whether the cable forces and the reaction force are positive. If all the above requirements are met, the point in the workspace is accepted as valid.

The variation in the robot's workspace for some of the valid values of angle θ is shown in Figure 9, which spans the current page and the following one. These points have been obtained based on the midpoint of segment $A_1 - A_3$ of the scraper because it is where the force F is applied (Figure 4), so it simplifies the calculation of static equilibrium.

To have a reference for the workspace with respect to the robot, Figure 8 represents the same workspace as in Figure 9a, but with the robot superimposed.

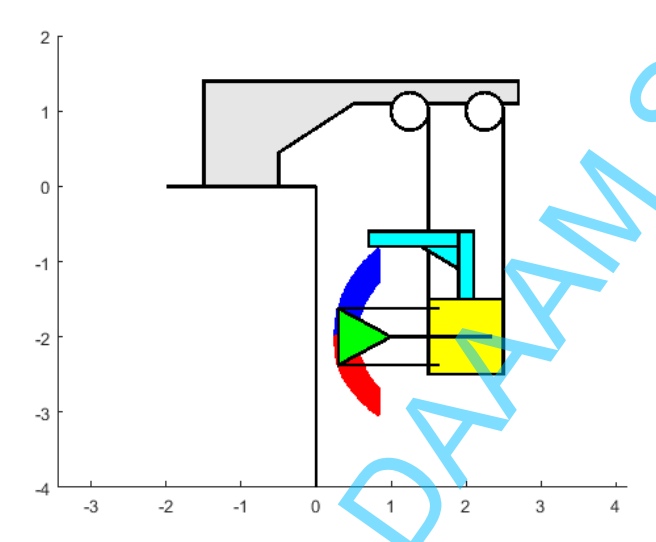
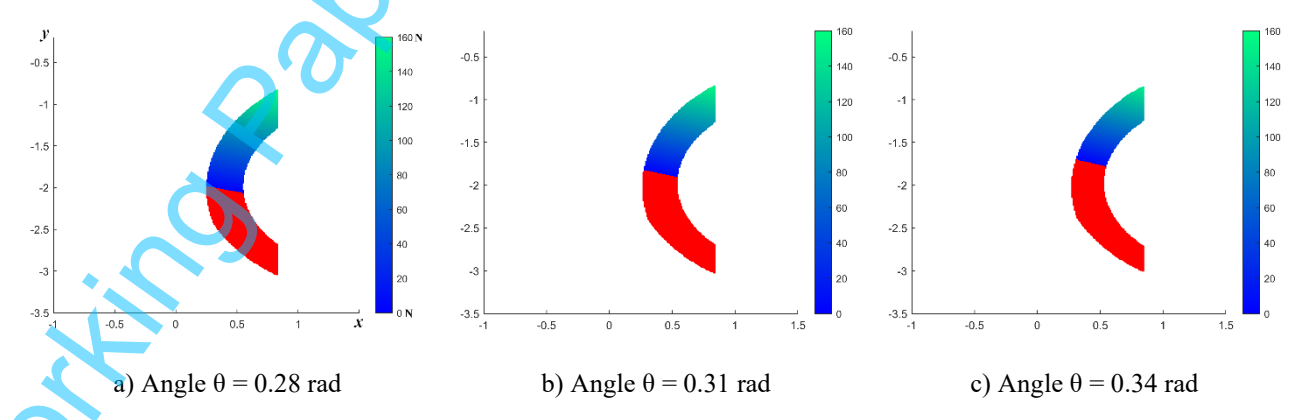


Fig. 8. Workspace and the plastering robot

Of all the points in the initial mesh (Figure 7), only those shown in Figure 9 are within the range of lengths of both actuators. Furthermore, of those points, only the blue and green ones also comply with the static equilibrium constraints.

It can be seen in the sequence of workspaces that, as the angle θ increases, the number of reachable points decreases and, among those that are reachable, there are increasingly those that do not meet the conditions of static equilibrium: points at which the tension forces in the cables or the reaction in the attachment arm become negative (red points).

Once the workspaces have been displayed, the force values obtained in the static equilibrium analysis ($F_{reaction}$, T_1 and T_2) will now be discussed. Since the value of these three variables is known at each point in the workspace, the intensity of the magnitude of these variables can be represented on the points of the workspace. Nevertheless, the values for the reaction force and tension T_1 will not be shown because their minimum values are 60 N and 270 N respectively, so they do not represent a stability problem for this robot. On the other hand, the T_2 tension does have values close to 0, being the most critical force. In fact, at the boundary between the points that do and do not satisfy the static equilibrium of forces (the boundary between the red and blue points), the tension values in the right cable are practically zero, indicating that it is this variable that prevents there being more valid points in the workspace. The magnitude, in Newtons, of the tension T_2 is expressed as a vertical-coloured bar in each of the subfigures in Figure 9.



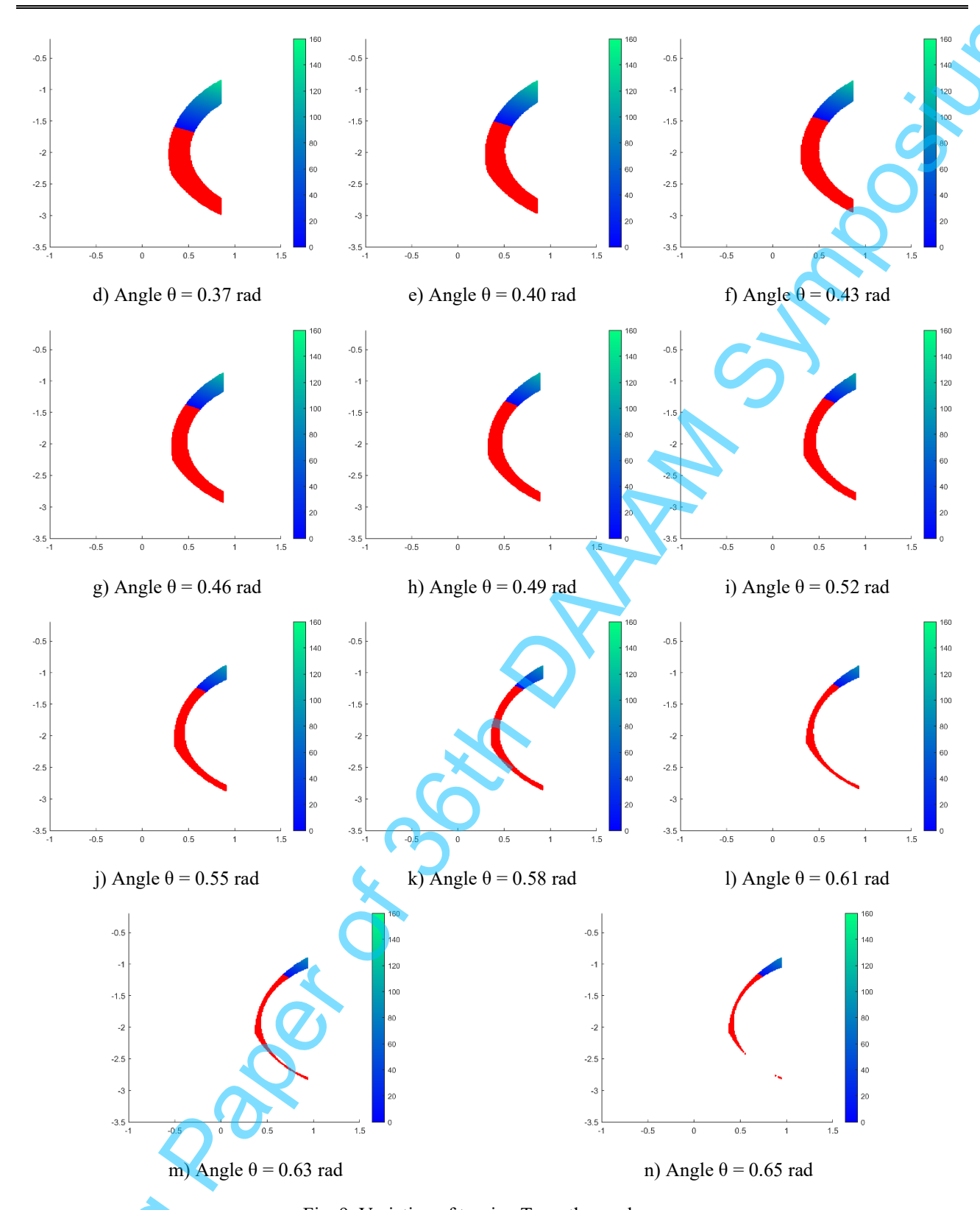


Fig. 9. Variation of tension T_2 on the workspace

Finally, the results of the singularity analysis are discussed. The magnitude of the value of the determinant of the robot's Jacobian matrix at all points in the workspace is always of the same sign (negative), which implies that there are no singular points for the studied orientations. This indicates that the design presented in this work avoids the appearance of singularities and, therefore, the robot will be able to move throughout its workspace without having to evade any area in which control may be lost due to singularities.

7. Conclusion

This paper presented the initial design and analysis of a new robot for plastering walls in the construction sector, an activity which, despite its apparent simplicity, involves significant risks for operators and presents technical challenges that have not yet been satisfactorily resolved by existing commercial solutions. The structural approach of this robot is different from that used by most current machines, which will allow it to be used effectively in environments where existing systems were not practical: walls too tall and walls without stable horizontal support at their bottom.

The analyses carried out in the previous sections have validated the feasibility of the proposed design for the plastering task and provide information that will be used to improve the current design of the robot. The results have shown that the robot can operate within an adequate workspace, without any singular point in it, and guarantee positive tension in the cables, which are essential conditions for its safe operation.

Future work will focus on refining the design and validating its performance in real conditions. More specifically, the next steps include designing an algorithm to calculate the optimal sequence of robot movements, improving the robot's design by optimizing the arrangement of joints, resizing the end effector, and modifying the geometry of certain parts, as well as constructing a prototype to carry out the necessary tests and verify the robot's performance in a controlled environment to ensure that it meets the desired specifications and performs the task correctly.

8. Acknowledgments

This work was supported by project PID2024-159765OA-I00, funded by State Research Agency of the Spanish Government.

9. References

- [1] Aghimien, D. O., Aigbavboa, C. O., Oke, A. E., & Thwala, W. D. (2020). Mapping out research focus for robotics and automation research in construction-related studies: A bibliometric approach. Journal of Engineering, Design and Technology, 18(5), 1063–1079. https://doi.org/10.1108/JEDT-09-2019-0237
- [2] Gharbia, M., Chang-Richards, A., Lu, Y., Zhong, R. Y., & Li, H. (2020). Robotic technologies for on-site building construction: A systematic review. Journal of Building Engineering, 32, 101584. https://doi.org/https://doi.org/10.1016/j.jobe.2020.101584
- [3] Akinlolu, M., Haupt, T. C., Edwards, D. J., & Simpeh, F. (2022). A bibliometric review of the status and emerging research trends in construction safety management technologies. International Journal of Construction Management, 22(14), 2699–2711. https://doi.org/10.1080/15623599.2020.1819584
- [4] Liu, Y., A.H., A., Haron, N. A., N.A., B., & Wang, H. (2024). Robotics in the Construction Sector: Trends, Advances, and Challenges. Journal of Intelligent & Robotic Systems, 110(2), 72. https://doi.org/10.1007/s10846-024-02104-4
- [5] Kim, M. J., Chi, H. L., Wang, X., & Ding, L. (2015). Automation and Robotics in Construction and Civil Engineering. Journal of Intelligent & Robotic Systems, 79(3-4), 347. https://doi.org/10.1007/s10846-015-0252-9
- [6] Pajaziti, A., Stuja, K., Gjelaj, A., & Calvin, L. (2023). Design and Optimization of the Welding Robot System for Aluminium Frames using Simulation Software, Proceedings of the 34th DAAAM International Symposium, pp.0040-0049, B. Katalinic (Ed.), Published by DAAAM International. ISBN 978-3-902734-41-9, ISSN 1726-9679, Vienna, Austria. DOI: 10.2507/34th.daaam.proceedings.006
- [7] Liu, Z., Chen, D., Eldosoky, M., Ye, Z., Jiang, X., Liu, Y., & Ge, S. (2024). Puttybot: A sensorized robot for autonomous putty plastering. Journal of Field Robotics, 41, 1744–1764. https://doi.org/10.1002/rob.22351
- [8] Bard, J., Bidgoli, A., & Chi, W. W. (2019). Image Classification for Robotic Plastering with Convolutional Neural Network. In J. Willmann, P. Block, M. Hutter, K. Byrne, & T. Schork (Eds.), Robotic Fabrication in Architecture, Art and Design 2018 (pp. 3–15). Springer International Publishing.
- [9] Forsberg, J., Graff, D., & Wernersson, Å. (1995). An Autonomous Plastering Robot for Walls and Ceilings. IFAC Proceedings Volumes, 28(11), 301–306. https://doi.org/https://doi.org/10.1016/S1474-6670(17)46989-8
- [10] Liu, G., Li, Z., Zhang, J., & Bao, H. (2024). A mortar scraping robot for a whole wall in construction. 2024 IEEE International Conference on Mechatronics and Automation (ICMA), 1688–1693.
- [11] Yadav, B., Mandal, N., Thakur, A., Jaiswal, B., Yadav, S., Pandit, S., Yadav, R., Shrestha, A., & Risal, S. (2020). International Journal of Advanced Engineering Modelling and Fabrication of Automatic Wall Plastering Machine.
- [12] Gosselin, C. M., & Sefrioui, J. (1991, June). Polynomial solutions for the direct kinematic problem of planar three-degree-of-freedom parallel manipulators. In Fifth International Conference on Advanced Robotics' Robots in Unstructured Environments (pp. 1124-1129). IEEE.
- [13] Wang, Y., Xie, L., Chen, J., Chen, M., Hu, T., Liao, H., Sun, S., & Chen, J. (2024). Mortar spraying and plastering integrated robot for wall construction. Automation in Construction, 165, 105533.